



CORRELATIONS OF SOLUTE PARTITIONING AND ENTHALPIES OF SOLVATION FOR ORGANIC SOLUTES IN IONIC LIQUIDS USING A TEMPERATURE INDEPENDENT FREE ENERGY RELATIONSHIP

Timothy W. Stephens^a, Bria Willis^a, Nishu Dabadge^a, Amy Tian^a, William E. Acree, Jr.^a,

Michael H. Abraham^b

Keywords: partition coefficient, 1-hexyl-3-methylimidazolium tetracyanoborate, 1-(2-methoxyethyl)-1-methylpiperidinium bis(trifluoromethylsulfonyl)imide and 1-(2-methoxyethyl)-1-methylpyrrolidinium bis(trifluoromethylsulfonyl)imide, ionic liquids, temperature independence, linear free energy relationships, enthalpies of solvation.

Experimental data have been collected from the published literature for the gas-to-ionic liquid partition coefficients and molar enthalpies of solvation for over 60 solutes in the ionic liquids 1-hexyl-3-methylimidazolium tetracyanoborate ([MHIm]⁺[B(CN)₄]⁻), 1-(2-methoxyethyl)-1-methylpiperidinium bis(trifluoromethylsulfonyl)imide ([MeoeMPip]⁺[Tf₂N]⁻), and 1-(2-methoxyethyl)-1-methylpyrrolidinium bis(trifluoromethylsulfonyl)imide ([MeoeMPyr]⁺[Tf₂N]⁻) over the temperature range 318.15 K to 368.15 K. The logarithm of the gas-to-ionic liquid partition coefficient, $\log K_L$, have been correlated to a temperature independent free energy relationship utilizing known Abraham solvation parameters. The resulting mathematical expressions describe the experimental $\log K_L$ values to within a standard deviation of 0.077 log units or less and ΔH_{solv} to within a standard deviation of 1.344 kJ mol⁻¹ or less.

* Corresponding Authors

Fax: 940-565-4318

E-Mail: acree@unt.edu

[a] Department of Chemistry, 1155 Union Circle Drive #305070, University of North Texas, Denton, TX 76203-5017 (USA)

[b] Department of Chemistry, University College London, 20 Gordon Street, London, WC1H 0AJ (UK)

Introduction

For over twenty years, room-temperature ionic liquids (RTILs) have been used in an ever growing area of study with regards to chemical separations. One of the most prominent features of ionic liquids is the ability to fine-tune and target specific solubilizing effects based on the choice of cation or anion, or even the side chains on the cation. The RTILs 1-(2-methoxyethyl)-1-methylpiperidinium bis(trifluoromethylsulfonyl)imide ([MeoeMPip]⁺[Tf₂N]⁻), and 1-(2-methoxyethyl)-1-methylpyrrolidinium bis(trifluoromethylsulfonyl)imide ([MeoeMPyr]⁺[Tf₂N]⁻), specifically the 2-methoxyethyl side chain, have both been shown to be particularly good at separations involving polar/non-polar azeotropic mixtures,^{1,2} while the RTIL 1-hexyl-3-methylimidazolium tetracyanoborate ([MHIm]⁺[B(CN)₄]⁻) has been shown to be very selective for aromatic and aliphatic hydrocarbons.³ RTILs that contain the anion [Tf₂N]⁻ have been shown to be completely immiscible with water while RTILs containing the cation [MHIm]⁺ have been shown to be partly soluble in water. These solubilizing characteristics allow for RTILs of this type to be used in liquid-liquid extractions between the RTIL and aqueous solution.

To date, the Abraham Solvation Parameter Model has been used to predict various solvation processes in a variety of types of solvent systems, including: the partitioning of solutes in polar organic solvents,⁴⁻⁹ the partitioning of solutes in non-polar organic solvents,¹⁰⁻¹² the partitioning

within micelles,^{13,14} solute partitioning within important biological systems,¹⁵⁻¹⁷ toxicity in aquatic organisms,¹⁸⁻²¹ solute partitioning in RTILs,²²⁻²⁷ and solute partitioning in binary solvent systems.²⁸ The Abraham Model can be written to predict the logarithm of the gas-to-solvent partition coefficient ($\log K_L$) and the logarithm of the water-to-solvent partition coefficient $\log P$, as shown in Eqns. 1 and 2 respectively. The Abraham Model has also been applied in the prediction of enthalpies of solvation,²⁹⁻³⁴ as shown in Eqn. 3.

$$\log K_L = c_K + e_K E + s_K S + a_K A + b_K B + l_K L \quad (1)$$

$$\log P = c_P + e_P E + s_P S + a_P A + b_P B + v_P V \quad (2)$$

$$\Delta H_{\text{solv}} = c_{H,\text{solv}} + e_{H,\text{solv}} E + s_{H,\text{solv}} S + a_{H,\text{solv}} A + b_{H,\text{solv}} B + l_{H,\text{solv}} L \quad (3)$$

Within the Abraham Model, the independent values are defined as solute-specific descriptor terms. These terms are defined as: E is the solute's excess molar refraction in units of 0.1 cm² mol⁻¹,³⁵ S is a measure of the solute's combined polarizability and dipolarity,³⁶ A is a measure of the solute's overall hydrogen-bond acidity,³⁷ B is a measure of the solute's overall hydrogen-bond basicity,³⁸ V is the solute's characteristic McGowan's molecular volume in units of 0.01 cm³ mol⁻¹,³⁹ and L is the logarithm of the solute's gas-to-hexadecane partition coefficient at 298 K.⁴⁰ The calculated coefficients c_K , e_K , s_K , a_K , b_K , l_K , c_P , e_P , s_P , a_P , b_P , v_P , $c_{H,\text{solv}}$, $e_{H,\text{solv}}$, $s_{H,\text{solv}}$, $a_{H,\text{solv}}$, $b_{H,\text{solv}}$, $l_{H,\text{solv}}$ have the following defined physico-chemical properties: e is a

measure of the solvent system's interactions with the solute's π - and non-bonding electrons, s is a measure of the solvent system's combined polarizability and dipolarity, a is a measure of the solvent system's hydrogen-bond basicity and is complimentary to the solute's hydrogen-bond acidity, b is a measure of the solvent system's hydrogen-bond acidity and is complimentary to the solute's hydrogen-bond basicity, and l and v are measures of general dispersion forces necessary to create a cavity in the solvent system for solubilizing the solute. When the solvent coefficients are combined with their complimentary descriptors, the resulting product can be used to characterize that particular solute-solvent interaction. For the partitioning between two condensed phases, the coefficient values can be used to indicate the differences between the two phases of that particular property.

Sprunger, et al.⁴¹⁻⁴³ have expanded the Abraham Model so that the gas-to-RTIL partition coefficient can be predicted based on ion-specific coefficients for individual cations and anions, as shown in Eqn. 4. Utilizing the ion-specific coefficients, RTILs can be synthesized that take advantage of specific properties that may be attractive for specific separations.

$$\log K_L = (c_{K,\text{cation}} + c_{K,\text{anion}}) + (e_{K,\text{cation}} + e_{K,\text{anion}}) E + (s_{K,\text{cation}} + s_{K,\text{anion}}) S + (a_{K,\text{cation}} + a_{K,\text{anion}}) A + (b_{K,\text{cation}} + b_{K,\text{anion}}) B + (l_{K,\text{cation}} + l_{K,\text{anion}}) L \quad (4)$$

Mintz, et al.⁴⁴ and Sprunger, et al.⁴⁵ describe a basis for incorporating temperature dependent terms into the Abraham Model that comes from the Gibbs' Free Energy Relationship, Eqn. 5, and the relation between ΔG_{solv} and K_L , Eqn. 6, where R is the universal gas constant in units of $\text{J mol}^{-1} \text{K}^{-1}$, T is the temperature of the system in Kelvin, and K_L is the gas-to-solvent partition coefficient.

$$\Delta G_{\text{solv}} = \Delta H_{\text{solv}} - T \Delta S_{\text{solv}} \quad (5)$$

$$\Delta G_{\text{solv}} = -RT \ln K_L \quad (6)$$

Converting Eqn. 6 from base e to base 10 so that the results correspond to previous Abraham Model correlations, yields Eqn. 7.

$$\Delta G_{\text{solv}} = -2.303 RT \log K_L \quad (7)$$

Using Eqns. 1, 3, 5 and 7, the Abraham Model can be applied to the prediction of ΔS_{solv} , expressed as Eqn. 8.

$$\Delta S_{\text{solv}} = c_{S,\text{solv}} + e_{S,\text{solv}} E + s_{S,\text{solv}} S + a_{S,\text{solv}} A + b_{S,\text{solv}} B + l_{S,\text{solv}} L \quad (8)$$

Eqns. 3, 5, 7, and 8 can now be combined and rewritten as Eqn. 9, and simplified into Eqn. 10.

$$-2.303 RT \log K_L = c_{H,\text{solv}} + e_{H,\text{solv}} E + s_{H,\text{solv}} S + a_{H,\text{solv}} A + b_{H,\text{solv}} B + l_{H,\text{solv}} L - T (c_{S,\text{solv}} + e_{S,\text{solv}} E + s_{S,\text{solv}} S + a_{S,\text{solv}} A + b_{S,\text{solv}} B + l_{S,\text{solv}} L) \quad (9)$$

$$\log K = \left(c_S - \frac{c_H}{T} \right) \frac{1}{2.303R} + \left(e_S - \frac{e_H}{T} \right) \frac{E}{2.303R} + \left(s_S - \frac{s_H}{T} \right) \frac{S}{2.303R} + \left(a_S - \frac{a_H}{T} \right) \frac{A}{2.303R} + \left(b_S - \frac{b_H}{T} \right) \frac{B}{2.303R} + \left(l_S - \frac{l_H}{T} \right) \frac{L}{2.303R} \quad (10)$$

Because of the relationship between $\log K_L$ and ΔH_{solv} , the c_H , e_H , s_H , a_H , b_H , and l_H coefficients from Eqn. 10 should yield the same coefficients as for Eqn. 3.

Data sets and computation methodology

Gas-to-solvent partition coefficients K_L were found for the RTILs 1-hexyl-3-methylimidazolium tetracyanoborate ($[\text{MHIIm}]^+[\text{B}(\text{CN})_4]^-$),³ 1-(2-methoxyethyl)-1-methylpiperidinium bis(trifluoromethylsulfonyl)imide ($[\text{MeoeMPip}]^+[\text{Tf}_2\text{N}]^-$),² and 1-(2-methoxyethyl)-1-methylpyrrolidinium bis(trifluoromethylsulfonyl)imide ($[\text{MeoeMPyrr}]^+[\text{Tf}_2\text{N}]^-$)¹ by performing a search of the chemical literature. All of the partition coefficients were converted to $\log K_L$ and tabulated with the necessary solute descriptors in a 12 column matrix. Enthalpies of solvation were calculated using the relationship given in Eqn. 11 and tabulated with the necessary solute descriptors into a 5 column matrix. A linear regression was performed on each matrix using the statistical software program SPSS 20.0. For the $\log K_L$ correlation, the linear regression was forced through the origin. For the ΔH_{solv} correlation, the linear regression was not forced through the origin.

$$\Delta H_{\text{solv}} = -2.303 R [\text{d} \log K_L / \text{d}(1/T)] \quad (11)$$

Table 1 lists all solute descriptors used for the analysis of the three RTILs. The solute descriptors used came from a database that the authors have compiled and were initially obtained using experimental data such as water-to-solvent partition coefficients, gas-to-solvent partition coefficients, solubility, and chromatographic data. Numerical values for the descriptors used in the analysis of the three ionic liquids cover the same area of predictive space, with values for each descriptor ranging from: $E = -0.063$ to $E = 0.851$, $S = 0.000$ to $S = 0.950$, $A = 0.000$ to $A = 0.820$, $B = 0.000$ to $B = 0.640$, and $L = 0.260$ to $L = 4.686$. The solutes used in each correlation show a wide range of functionality as well as non-polar and polar characteristics. For all correlations, the authors report the N (number of data points), R^2 (square of the correlation coefficient), F (Fisher's F-Statistic), and SD (standard deviation).

Table 1. Solute descriptors used in the analyses

Solute	<i>E</i>	<i>S</i>	<i>A</i>	<i>B</i>	<i>L</i>
Pentane	0.000	0.000	0.000	0.000	2.162
Hexane	0.000	0.000	0.000	0.000	2.668
3-Methylpentane	0.000	0.000	0.000	0.000	2.581
2,2-Dimethylbutane	0.000	0.000	0.000	0.000	2.352
Heptane	0.000	0.000	0.000	0.000	3.173
Octane	0.000	0.000	0.000	0.000	3.677
2,2,4-trimethylpentane	0.000	0.000	0.000	0.000	3.106
Nonane	0.000	0.000	0.000	0.000	4.182
Decane	0.000	0.000	0.000	0.000	4.686
Cyclopentane	0.263	0.100	0.000	0.000	2.477
Cyclohexane	0.310	0.100	0.000	0.000	2.964
Methylcyclohexane	0.244	0.060	0.000	0.000	3.319
Cycloheptane	0.350	0.100	0.000	0.000	3.704
Cyclooctane	0.413	0.100	0.000	0.000	4.329
Pent-1-ene	0.093	0.080	0.000	0.070	2.047
Hex-1-ene	0.080	0.080	0.000	0.070	2.572
Cyclohexene	0.395	0.280	0.000	0.090	2.952
Hept-1-ene	0.092	0.080	0.000	0.070	3.063
Oct-1-ene	0.090	0.080	0.000	0.070	3.568
Dec-1-ene	0.093	0.080	0.000	0.070	4.554
Hex-1-yne	0.166	0.220	0.100	0.120	2.510
Hept-1-yne	0.160	0.230	0.090	0.100	3.000
Oct-1-yne	0.155	0.220	0.090	0.100	3.521
Benzene	0.610	0.520	0.000	0.140	2.786
Toluene	0.601	0.520	0.000	0.140	3.325
Ethylbenzene	0.613	0.510	0.000	0.150	3.778
<i>o</i> -Xylene	0.663	0.560	0.000	0.160	3.939
<i>m</i> -Xylene	0.623	0.520	0.000	0.160	3.839
<i>p</i> -Xylene	0.613	0.520	0.000	0.160	3.839
Styrene	0.849	0.650	0.000	0.160	3.856
α -Methylstyrene	0.851	0.640	0.000	0.190	4.290
Thiophene	0.687	0.570	0.000	0.150	2.819
Methanol	0.278	0.440	0.430	0.470	0.970
Ethanol	0.246	0.420	0.370	0.480	1.485
Propan-1-ol	0.236	0.420	0.370	0.480	2.031
Propan-2-ol	0.212	0.360	0.330	0.560	1.764
Butan-1-ol	0.224	0.420	0.370	0.480	2.601
Butan-2-ol	0.217	0.360	0.330	0.560	2.338
2-Methyl-1-propanol	0.217	0.390	0.370	0.480	2.413
<i>tert</i> -Butanol	0.180	0.300	0.310	0.600	1.963
Water	0.000	0.600	0.590	0.460	0.245
Acetic acid	0.265	0.640	0.620	0.440	1.816
Tetrahydrofuran	0.289	0.520	0.000	0.480	2.636
1,4-Dioxane	0.329	0.750	0.000	0.640	2.892
<i>tert</i> -Butyl methyl ether	0.024	0.220	0.000	0.550	2.372
<i>tert</i> -Butyl ethyl ether	-0.020	0.160	0.000	0.600	2.720
<i>tert</i> -Amyl methyl ether	0.050	0.210	0.000	0.600	2.916
Diethyl ether	0.041	0.250	0.000	0.450	2.015
Dipropyl ether	0.008	0.250	0.000	0.450	2.954
Diisopropyl ether	-0.063	0.170	0.000	0.570	2.501
Dibutyl ether	0.000	0.250	0.000	0.450	3.924
Acetone	0.179	0.700	0.040	0.490	1.696
Pentan-2-one	0.143	0.680	0.000	0.510	2.755
Pentan-3-one	0.154	0.660	0.000	0.510	2.811
Methyl acetate	0.142	0.640	0.000	0.450	1.911
Ethyl acetate	0.106	0.620	0.000	0.450	2.314

Methyl propanoate	0.128	0.600	0.000	0.450	2.431
Methyl butanoate	0.106	0.600	0.000	0.450	2.893
Butanal	0.187	0.650	0.000	0.450	2.270
Acetonitrile	0.237	0.900	0.070	0.320	1.739
Pyridine	0.631	0.840	0.000	0.520	3.022
1-Nitropropane	0.242	0.950	0.000	0.310	2.894

RESULTS AND DISCUSSION

Values for $\log K_L$ and ΔH_{solv} have been assembled and tabulated in Table 2 for the partitioning of 61 solutes in ([MHIm]⁺[B(CN)₄]⁻) over the temperature range of 318.15 K to 368.15 K. A regression analysis of the entire data set listed in Table 2 yielded Eqns. 12 and 13. Figure 1 is presented as a comparison of the experimental $\log K_L$ values from Table 2 and the calculated $\log K_L$ from Eqn. 12.

$$\log K_L = -7.641(0.471)/(2.303R) + [16.206(10.807) - (5233(3708)/T)][E/(2.303R)] + [-15.729(10.624) - (-19911(3644)/T)][S/(2.303R)] + [-37.872(10.466) - (25751(3587)/T)][A/(2.303R)] + [-8.254(10.711) - (-4842(3668)/T)][B/(2.303R)] + [-14.280(0.935) - (-8336(316)/T)][L/(2.303R)] \quad (12)$$

$$N = 361, R^2 = 0.999, F = 25965, SD = 0.077 \text{ log units}$$

$$\Delta H_{\text{solv}} = 4098(1159) E - 17444(1147) S - 24979(1142) A - 6532(1181) B - 8313(104) L \quad (13)$$

$$N = 61, R^2 = 0.998, F = 6880, SD = 1344 \text{ J mol}^{-1}$$

For these correlations, the ΔH_{solv} data was converted from kJ mol⁻¹ to J mol⁻¹ so that a comparison of the c_H , e_H , s_H , a_H , b_H and l_H coefficients from Eqn. 12 could be made to the $c_{H,\text{solv}}$, $e_{H,\text{solv}}$, $s_{H,\text{solv}}$, $a_{H,\text{solv}}$, $b_{H,\text{solv}}$ and $l_{H,\text{solv}}$ coefficients from Eqn. 13. During the analysis of the $\log K_L$ data, it was found that the c_S coefficient had a linear covariance and was thus excluded from the regression. When the c_H term from the original $\log K_L$ correlation was compared to the original $c_{H,\text{solv}}$ term from the original ΔH_{solv} correlation, the two terms were not in agreement with each other. Therefore, a new regression was calculated for $\log K_L$ which excluded the c_H term, presented as Eqn. 12, and a new regression was calculated for ΔH_{solv} which excluded the $c_{H,\text{solv}}$ term, presented as Eqn. 13.

Eqn. 14 was derived by writing the e_H , s_H , a_H , b_H and l_H coefficients from Eqn. 12 to predict ΔH_{solv} .

$$\Delta H_{\text{solv}} = 5233(3708) E - 19911(3644) S - 25751(3587) A -$$

$$4842(3688) B - 8336(316) L \quad (14)$$

$$SD = 1424 \text{ J mol}^{-1}, AAE = 1064 \text{ J mol}^{-1}, AE = 192 \text{ J mol}^{-1}$$

Reported are the SD , AAE (absolute average error), and AE (average error) for the prediction of ΔH_{solv} based on Eqn. 14. As shown, Eqn. 14 predicts ΔH_{solv} to within a similar standard deviation as Eqn. 13. The very low AE and AAE values show very little bias between using Eqn. 13 or Eqn. 14 to predict ΔH_{solv} . Eqn. 14 also illustrates that the e_{H} , s_{H} , a_{H} , b_{H} and l_{H} coefficients from Eqn. 12 and the $e_{\text{H,solv}}$, $s_{\text{H,solv}}$, $a_{\text{H,solv}}$, $b_{\text{H,solv}}$ and $l_{\text{H,solv}}$ coefficients from Eqn. 13 are individually within the statistical error of their respective counterparts.

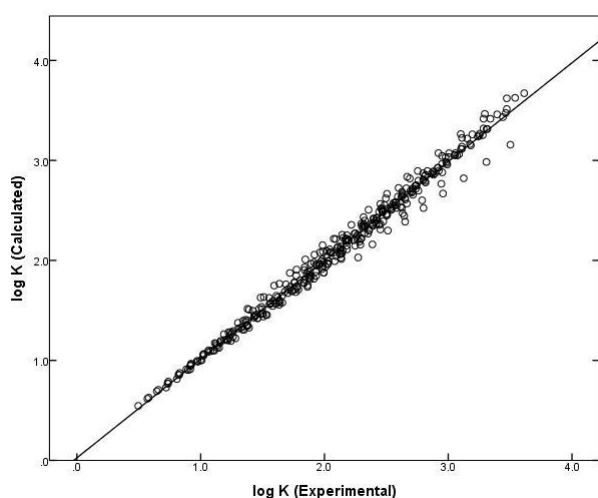


Figure 1. Graph of experimental logarithm of gas-to- $[\text{MHIm}]^+[\text{B}(\text{CN})_4]^-$ partition coefficient ($\log K_L$) versus calculated $\log K_L$ based on Eq. 12.

As an informational note one could develop Abraham model correlations for each individual temperature. As noted by Mintz et al.⁴⁴ and Sprunger et al.⁴⁵ offers over such temperature-specific correlations is that one can develop correlations for more partitioning process and for more ionic liquid solvents. For example, let's assume that one was able to find $\log K_L$ data 20 solutes in $([\text{MHIm}]^+[\text{B}(\text{CN})_4]^-)$ at 298 K, $\log K_L$ data for a different set of 20 solutes in $([\text{MHIm}]^+[\text{B}(\text{CN})_4]^-)$ at 318.15 K, and $\log K_L$ data for a third set of 20 different solutes in $([\text{MHIm}]^+[\text{B}(\text{CN})_4]^-)$ at 368 K. There would be insufficient experimental data to develop a meaningful Abraham model correlation at any of the three temperatures mentioned. However, by pooling the 60 $\log K_L$ values for $([\text{MHIm}]^+[\text{B}(\text{CN})_4]^-)$ into a single dataset, one could develop a predictive correlation based on Eqn. 10. Such predictions would not be possible with Eqn. 1 which requires that all of the experimental data be at the same temperature.

To determine the predictability of Eqn. 12, the data in Table 2 was analyzed using a training set and test analysis. In this method of analysis, the complete data set is randomly split in half and divided into a training set and a test set. In the event that the complete data set has an odd number of data points, the extra data point is included in the training set. A linear regression is then performed on the training set and a new training correlation is calculated. This training

correlation is then used to predict the values in the test set, and the SD , AAE , and AE are reported. Eqn. 15 is the resultant correlation from randomly splitting half of the $\log K_L$ data reported in Table 2. Using Eqn. 15 to predict the values in the test set yielded a $SD = 0.083$ log units, $AAE = 0.055$, and $AE = -0.004$. The very small difference in the coefficient values calculated between the training set and parent set show that the training set compounds and temperatures are representative of the parent compounds and temperatures. The low AE value shows very little bias between using Eqns. 12 and 15.

$$\begin{aligned} \log K_L = & -7.699(0.653)/(2,303 R) + \\ & [15.446(14.979) - (4914(5133)/T)] [E/(2.303 R)] + \\ & [-14.226(15.704) - (-19294(5388)/T)] [S/(2.303 R)] + \\ & [-58.028(17.935) - (-33067(6232)/T)] [A/(2.303 R)] + \\ & [-9.661(15.007) - (-5405(5189)/T)] [B/(2.303 R)] + \\ & [-14.012(1.297) - (-8245(445)/T)] [L/(2.303 R)] \quad (15) \end{aligned}$$

$$N = 181, R^2 = 0.999, F = 13690, SD = 0.074 \text{ log units}$$

Values for $\log K_L$ and ΔH_{solv} have been assembled and tabulated in Table 3 for the partitioning of 61 solutes in $([\text{MeoeMPip}]^+[\text{Tf}_2\text{N}]^-)$ over the temperature range of 318.15 K to 368.15 K. A regression analysis of the entire data set listed in Table 3 yielded Eqns. 16 and 17. Figure 2 is presented as a comparison of the experimental $\log K_L$ values from Table 3 and the calculated $\log K_L$ from Eqn. 16.

$$\begin{aligned} \log K_L = & -10.878(0.387)/(2.303 R) + \\ & [0.536(6.437) - (-14440(2202)/T)] [S/(2.303 R)] + \\ & [-29.947(9.729) - (-23020(3325)/T)] [A/(2.303 R)] + \\ & [-17.927(7.920) - (-7332(2707)/T)] [B/(2.303 R)] + \\ & [-12.721(0.706) - (-7802(239)/T)] [L/(2.303 R)] \quad (16) \end{aligned}$$

$$N = 365, R^2 = 0.999, F = 31686, SD = 0.069 \text{ log units}$$

$$\begin{aligned} \Delta H_{\text{solv}} = & -14486(805) S - 22955(1223) A - \\ & 7248(991) B - 7791(88) L \quad (17) \end{aligned}$$

$$N = 61, R^2 = 0.998, F = 7868, SD = 1335 \text{ J/mol}$$

For these correlations, the ΔH_{solv} data was converted from kJ mol^{-1} to J mol^{-1} so that a comparison of the c_{H} , e_{H} , s_{H} , a_{H} , b_{H} and l_{H} coefficients from Eqn. 16 could be made to the $c_{\text{H,solv}}$, $e_{\text{H,solv}}$, $s_{\text{H,solv}}$, $a_{\text{H,solv}}$, $b_{\text{H,solv}}$ and $l_{\text{H,solv}}$ coefficients from Eqn. 17. Coincidentally, during the analysis of the $\log K_L$ data for $([\text{MeoeMPip}]^+[\text{Tf}_2\text{N}]^-)$, it was found that the c_{S} coefficient was found to have a linear covariance and was thus excluded from the regression. When the c_{H} term from

the original $\log K_L$ correlation was compared to the original $c_{H,solv}$ term from the original ΔH_{solv} correlation, the two terms were also not in agreement with each other, as occurred for $([MHIm]^+[B(CN)_4]^-)$. Further analysis of the correlation for $\log K_L$ showed that the e_S and e_H terms were very small, 9.267(8.538) and 1986(2921) respectively. These terms were subsequently set equal to zero and the regression was performed once again. Eqn. 16 is the resultant correlation obtained by removing the c_H , e_S and e_H terms and Eqn. 17 is the resultant correlation obtained when the $c_{H,solv}$ and $e_{H,solv}$ terms are removed.

Eqn. 18 was derived by writing the s_H , a_H , b_H and l_H coefficients from Eqn. 16 to predict ΔH_{solv} .

$$\Delta H_{solv} = -14440(2202) S - 23020(3325) A - 7332(2707) B - 7802(239) L \quad (18)$$

$$SD = 1335 \text{ J mol}^{-1}, AAE = 1011 \text{ J mol}^{-1}, AE = -93 \text{ J mol}^{-1}.$$

Reported are the SD , AAE , and AE for the prediction of ΔH_{solv} based on Eqn. 18. As shown, Eqn. 18 predicts ΔH_{solv} to within the same standard deviation as Eqn. 17. The very low AE and AAE values show very little bias between using Eqn. 17 or Eqn. 18 to predict ΔH_{solv} . Eqn. 18 also illustrates that the s_H , a_H , b_H and l_H coefficients from Eqn. 16 and the $s_{H,solv}$, $a_{H,solv}$, $b_{H,solv}$ and $l_{H,solv}$ coefficients from Eqn. 17 are individually within the statistical error of their respective counterparts.

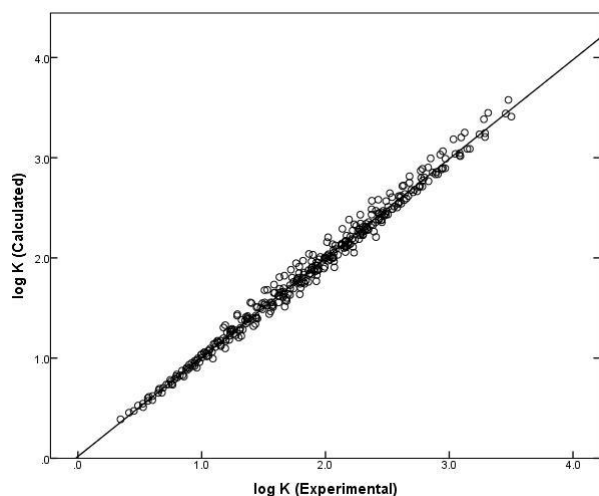


Figure 2. Graph of experimental logarithm of gas-to- $([MeoeMPip]^+[Tf_2N]^-)$ partition coefficient ($\log K_L$) versus calculated $\log K_L$ based on Eqn. 16.

To determine the predictability of Eqn. 16, the data in Table 3 was also analyzed using a training set and test analysis. Eqn. 19 is the resultant correlation from randomly splitting half of the $\log K_L$ data reported in Table 3. Using Eqn. 19 to predict the values in the test set yielded a $SD = 0.071$ log units, $AAE = 0.053$, and $AE = 0.002$.

The very small difference in the coefficient values calculated between the training set and parent set show that the training set compounds and temperatures are representative of the parent compounds and temperatures. The low AE value shows very little bias between using Eqns. 16 and 19.

$$\begin{aligned} \log K_L = & -10.992(0.562)/(2.303 R) + \\ & [5.061(9.173) - (-12834(3131)/T)] [S/(2.303 R)] + \\ & [-16.206(14.399) - (-18341(4871)/T)] [A/(2.303 R)] + \\ & [-27.181(12.155) - (-10547(4150)/T)] [B/(2.303 R)] + \\ & [-12.610(0.926) - (-7777(307)/T)] [L/(2.303 R)] \end{aligned} \quad (19)$$

$$N = 183, R^2 = 0.999, F = 17102, SD = 0.068 \text{ log units}$$

It should be noted that Marciniak and Wlazło² also correlated the $\log K_L$ data for $([MeoeMPip]^+[Tf_2N]^-)$ in terms of the Abraham model. The authors developed temperature-specific correlations in the form of Eqn. 1 for each of the six temperatures studied. A total of 36 curve-fit equation coefficients were needed to describe the 365 experimental data points to an average standard deviation of $SD = 0.059$ log units. Our method, Eqn. 16, has only nine curve-fit equation coefficients and describes the 365 $\log K_L$ values to within $SD = 0.069$ log units. Very little loss in predictive ability resulted from our method of combining all 365 experimental values into a single regression analysis.

Values for $\log K_L$ and ΔH_{solv} have been assembled and tabulated in Table 4 for the partitioning of 61 solutes in $([MeoeMPyr]^+[Tf_2N]^-)$ over the temperature range of 318.15 K to 368.15 K. A regression analysis of the entire data set listed in Table 4 yielded Eqns. 20 and 21. Figure 3 is presented as a comparison of the experimental $\log K_L$ values from Table 4 and the calculated $\log K_L$ from Eqn. 20.

$$\begin{aligned} \log K_L = & -10.033(0.375)/(2.303 R) + \\ & [10.075(8.499) - (2557(2905)/T)] [E/(2.303 R)] + \\ & [-7.117(8.475) - (-16471(2897)/T)] [S/(2.303 R)] + \\ & [-33.881(9.165) - (-24144(3132)/T)] [A/(2.303 R)] + \\ & [-12.474(8.752) - (-6027(2992)/T)] [B/(2.303 R)] + \\ & [-13.508(0.763) - (-7875(258)/T)] [L/(2.303 R)] \end{aligned} \quad (20)$$

$$N = 366, R^2 = 0.999, F = 30869, SD = 0.064 \text{ log units}$$

$$\begin{aligned} \Delta H_{solv} = & -2534(1090) E - 16481(1086) S - \\ & 24066(1175) A - 5998(1123) B - 7856(97) L \end{aligned} \quad (21)$$

$$N = 61, R^2 = 0.998, F = 6976, SD = 1260 \text{ J/mol}$$

For these correlations, the ΔH_{solv} data was converted from kJ mol^{-1} to J mol^{-1} so that a comparison of the c_H , e_H , s_H , a_H , b_H and l_H coefficients from Eqn. 20 could be made to the $c_{H,solv}$, $e_{H,solv}$, $s_{H,solv}$, $a_{H,solv}$, $b_{H,solv}$ and $l_{H,solv}$ coefficients from Eqn. 21. Coincidentally, during the analysis of the $\log K_L$ data for $([MeoeMPyr]^+[Tf_2N]^-)$, it was found that the c_S coefficient was found to have a linear covariance and was

thus excluded from the regression. When the c_H term from the original $\log K_L$ correlation was compared to the original $c_{H,solv}$ term from the original ΔH_{solv} correlation, the two terms were also not in agreement with each other, as occurred for $([MHIm]^+[B(CN)_4]^-)$ and $([MeoeMPip]^+[Tf_2N]^-)$. Once again, Eqn. 20 is the resultant correlation obtained by removing the c_H term and Eqn. 21 is the resultant correlation obtained when the $c_{H,solv}$ term is removed.

Eqn. 22 was derived by writing the e_H , s_H , a_H , b_H , and l_H coefficients from Eqn. 20 to predict ΔH_{solv} .

$$\Delta H_{solv} = 2557(2905) E - 16471(2897) S -$$

$$24144(3132) A - 6027(2992) B - 7875(258) L \quad (22)$$

$$SD = 1263 \text{ J mol}^{-1}, AAE = 1005 \text{ J mol}^{-1}, AE = -7 \text{ J mol}^{-1}$$

Reported are the SD , AAE , and AE for the prediction of ΔH_{solv} based on Eqn. 22. As shown, Eqn. 22 predicts ΔH_{solv} to within a similar standard deviation as Eqn. 21. The very low AE and AAE values show very little bias between using Eqn. 21 or Eqn. 22 to predict ΔH_{solv} . Eqn. 22 also illustrates that the e_H , s_H , a_H , b_H and l_H coefficients from Eqn. 20 and the $c_{H,solv}$, $e_{H,solv}$, $s_{H,solv}$, $a_{H,solv}$, $b_{H,solv}$ and $l_{H,solv}$ coefficients from Eqn. 21 are individually within the statistical error of their respective counterparts.

Table 2. Logarithm of gas-to- $([MHIm]^+[B(CN)_4]^-)$ partition coefficients at various temperatures and enthalpies of solvation (in kJ mol^{-1})^a

Solute Temperature, K	$\log K_L$						ΔH_{solv} kJ mol ⁻¹
	318.15	328.15	338.15	348.15	358.15	368.15	
Pentane	0.917	0.820	0.732	0.645	0.569	0.496	-18.887
Hexane	1.246	1.130	1.021	0.919	0.827	0.736	-22.814
3-Methylpentane	1.215	1.100	0.997	0.898	0.808	0.720	-22.131
2,2-Dimethylbutane	1.025	0.923	0.830	0.739	0.658	0.580	-19.965
Heptane	1.567	1.431	1.305	1.188	1.079	0.977	-26.423
Octane	1.884	1.728	1.583	1.446	1.322	1.204	-30.448
2,2,4-Trimethylpentane	1.491	1.362	1.241	1.124	1.021	0.922	-25.547
Nonane	2.196	2.021	1.857	1.703	1.565	1.431	-34.262
Decane	2.508	2.310	2.130	1.959	1.805	1.658	-38.033
Cyclopentane	1.365	1.255	1.155	1.057	0.970	0.885	-21.531
Cyclohexane	1.679	1.555	1.439	1.332	1.228	1.134	-24.481
Methylcyclohexane	1.840	1.704	1.581	1.459	1.350	1.246	-26.650
Cycloheptane	2.179	2.033	1.892	1.760	1.640	1.526	-29.312
Cyclooctane	2.615	2.442	2.283	2.134	1.994	1.863	-33.670
Hex-1-ene	1.459	1.336	1.220	1.111	1.009	0.915	-24.433
Cyclohexene	1.985	1.846	1.720	1.593	1.484	1.378	-27.185
Hept-1-ene	1.779	1.634	1.501	1.375	1.260	1.149	-28.194
Oct-1-ene	2.093	1.930	1.777	1.633	1.504	1.380	-31.974
Dec-1-ene	2.714	2.508	2.324	2.146	1.985	1.832	-39.487
Hex-1-yne	2.029	1.879	1.740	1.606	1.486	1.371	-29.510
Hept-1-yne	2.352	2.182	2.025	1.873	1.736	1.607	-33.403
Oct-1-yne	2.666	2.476	2.299	2.130	1.980	1.836	-37.206
Benzene	2.629	2.471	2.320	2.182	2.053	1.931	-31.295
Toluene	2.982	2.801	2.629	2.473	2.326	2.188	-35.599
Ethylbenzene	3.252	3.053	2.866	2.695	2.534	2.384	-38.901
o-Xylene	3.464	3.254	3.058	2.879	2.710	2.553	-40.820
m-Xylene	3.316	3.110	2.919	2.744	2.579	2.425	-39.887
p-Xylene	3.310	3.103	2.915	2.737	2.574	2.420	-39.850
Styrene		3.441	3.239	3.052	2.878	2.715	-41.945
α -Methylstyrene		3.614	3.395	3.195	3.007	2.831	-45.191
Methanol	2.400	2.250	2.111	1.984	1.865	1.757	-28.807
Ethanol	2.582	2.418	2.267	2.127	1.994	1.874	-31.737
Propan-1-ol	2.925	2.739	2.569	2.408	2.260	2.127	-35.771
Propan-2-ol	2.625	2.452	2.292	2.143	2.009	1.884	-33.194
Butan-1-ol	3.279	3.072	2.880	2.703	2.542	2.391	-39.749
Butan-2-ol	2.952	2.759	2.582	2.417	2.267	2.127	-36.920
2-Methyl-1-propanol	3.087	2.891	2.708	2.539	2.384	2.238	-38.043
tert-Butanol	2.631	2.452	2.290	2.137	1.993	1.864	-34.386
Water	2.668	2.505	2.356	2.217	2.090	1.964	-31.458
Acetic acid		3.540	3.340	3.153	2.979	2.816	-41.860
Solute	$\log K_L$						ΔH_{solv}

Temperature, K	318.15	kJ mol^{-1}	338.15	348.15	358.15	368.15	kJ mol^{-1}
Thiophene	2.759	2.593	2.441	2.301	2.167	2.045	-31.953
Tetrahydrofuran	2.626	2.465	2.318	2.179	2.053	1.935	-30.959
1,4-Dioxane	3.295	3.101	2.921	2.754	2.599	2.452	-37.775
tert-Butyl methyl ether	1.914	1.768	1.634	1.507	1.391	1.281	-28.346
tert-Butyl ethyl ether	1.839	1.689	1.553	1.422	1.301	1.188	-29.186
tert-Amyl methyl ether	2.248	2.083	1.933	1.790	1.660	1.535	-31.894
Diethyl ether	1.623	1.496	1.378	1.265	1.161	1.064	-25.063
Dipropyl ether	2.076	1.920	1.775	1.636	1.511	1.391	-30.694
Diisopropyl ether	1.759	1.612	1.473	1.342	1.225	1.114	-28.922
Dibutyl ether	2.689	2.496	2.316	2.143	1.987	1.839	-38.115
Acetone	2.621	2.468	2.326	2.196	2.072	1.958	-29.707
Pentan-2-one	3.176	2.987	2.813	2.650	2.501	2.360	-36.526
Pentan-3-one	3.182	2.993	2.816	2.652	2.502	2.360	-36.822
Methyl acetate	2.456	2.299	2.152	2.021	1.893	1.773	-30.557
Ethyl acetate	2.661	2.486	2.326	2.182	2.041	1.915	-33.372
Methyl propanoate	2.735	2.559	2.394	2.243	2.104	1.975	-34.044
Methyl butanoate	3.002	2.810	2.630	2.467	2.316	2.173	-37.080
Butanal	2.944	2.789	2.644	2.512	2.387	2.272	-30.120
Acetonitrile	3.502	3.309	3.125	2.958	2.800	2.651	-38.133
Pyridine		3.473	3.285	3.111	2.950	2.797	-39.012
1-Nitropropane		3.473	3.285	3.111	2.950	2.797	-39.012

^a Experimental gas-to-liquid partition coefficient data taken from Domańska et al.³

Table 3. Logarithm of gas-to-([MeoMPip]⁺[Tf₂N]⁻) partition coefficients at various temperatures and enthalpies of solvation (in kJ mol^{-1})^a

Solute Temperature, K	$\log K_L$						ΔH_{solv} kJ mol^{-1}
	318.15 K	328.15 K	338.15 K	348.15 K	358.15 K	368.15 K	
Pentane	0.751	0.653	0.565	0.486	0.413	0.344	-18.120
Hexane	1.061	0.944	0.841	0.746	0.658	0.574	-21.706
3-Methylpentane	1.041	0.926	0.824	0.732	0.648	0.566	-21.169
2,2-Dimethylbutane	0.884	0.780	0.688	0.604	0.525	0.452	-19.293
Heptane	1.365	1.230	1.111	0.999	0.899	0.798	-25.292
Octane	1.662	1.509	1.371	1.246	1.127	1.021	-28.653
2,2,4-Trimethylpentane	1.360	1.228	1.111	1.000	0.901	0.804	-24.804
Nonane	1.958	1.785	1.630	1.490	1.358	1.236	-32.259
Decane	2.248	2.057	1.888	1.730	1.583	1.444	-35.887
Cyclopentane	1.176	1.068	0.969	0.879	0.794	0.714	-20.638
Cyclohexane	1.476	1.350	1.238	1.134	1.037	0.947	-23.604
Methylcyclohexane	1.627	1.491	1.369	1.260	1.155	1.057	-25.445
Cycloheptane	1.926	1.780	1.645	1.524	1.413	1.307	-27.621
Cyclooctane	2.326	2.161	2.009	1.870	1.742	1.621	-31.537
Pent-1-ene	0.961	0.857	0.765	0.679	0.601	0.526	-19.393
Hex-1-ene	1.274	1.155	1.041	0.943	0.846	0.758	-23.104
Cyclohexene	1.763	1.628	1.508	1.393	1.288	1.190	-25.619
Hept-1-ene	1.579	1.438	1.307	1.193	1.083	0.983	-26.638
Oct-1-ene	1.876	1.716	1.569	1.438	1.312	1.196	-30.392
Dec-1-ene	2.458	2.262	2.083	1.919	1.765	1.618	-37.540
Hex-1-yne	1.862	1.713	1.576	1.450	1.332	1.223	-28.601
Hept-1-yne	2.161	1.995	1.841	1.699	1.566	1.442	-32.200
Oct-1-yne	2.456	2.272	2.100	1.943	1.795	1.658	-35.754
Benzene	2.505	2.348	2.201	2.064	1.941	1.825	-30.493
Toluene	2.833	2.654	2.489	2.336	2.193	2.061	-34.568
Ethylbenzene	3.084	2.889	2.708	2.539	2.384	2.238	-37.904
<i>o</i> -Xylene	3.289	3.085	2.895	2.719	2.556	2.403	-39.667
<i>m</i> -Xylene	3.166	2.967	2.783	2.612	2.452	2.303	-38.658
<i>p</i> -Xylene	3.146	2.945	2.760	2.589	2.430	2.279	-38.806
Styrene	3.502	3.289	3.090	2.908	2.740	2.580	-41.258
α -Methylstyrene		3.457	3.244	3.050	2.866	2.693	-44.091
Thiophene	2.636	2.473	2.322	2.182	2.053	1.932	-31.538
Solute	$\log K_L$						ΔH_{solv}

Temperature, K	318.15 K	318.15 K	318.15 K	318.15 K	318.15 K	318.15 K	kJ mol ⁻¹
Pyridine	3.314	3.125	2.948	2.784	2.631	2.490	-36.943
Methanol	2.158	2.017	1.887	1.770	1.660	1.556	-26.906
Ethanol	2.336	2.182	2.037	1.906	1.781	1.665	-30.082
Propan-1-ol	2.640	2.465	2.303	2.158	2.017	1.889	-33.637
Propan-2-ol	2.391	2.223	2.068	1.930	1.800	1.679	-31.795
Butan-1-ol	2.970	2.773	2.592	2.428	2.274	2.134	-37.420
Butan-2-ol	2.669	2.481	2.316	2.161	2.021	1.889	-34.815
2-Methyl-propan-1-ol	2.799	2.607	2.431	2.274	2.127	1.992	-36.095
tert-Butanol	2.408	2.230	2.072	1.926	1.792	1.671	-32.935
Water	2.427	2.281	2.137	2.013	1.898	1.788	-28.590
Methyl acetate	2.288	2.134	1.993	1.862	1.742	1.630	-29.419
Methyl propanoate	2.542	2.371	2.215	2.068	1.936	1.811	-32.713
Methyl butanoate	2.786	2.602	2.433	2.274	2.130	1.994	-35.447
Ethyl acetate	2.493	2.324	2.167	2.025	1.893	1.770	-32.340
Tetrahydrofuran	2.373	2.220	2.079	1.948	1.827	1.714	-29.489
1,4-Dioxane	3.034	2.850	2.679	2.520	2.373	2.233	-35.879
tert-Butyl methyl ether	1.686	1.545	1.418	1.299	1.190	1.090	-26.666
tert-Butyl ethyl ether	1.590	1.450	1.322	1.204	1.097	0.994	-26.629
tert-Amyl methyl ether	1.986	1.831	1.688	1.556	1.435	1.320	-29.814
Diethyl ether	1.380	1.262	1.152	1.053	0.959	0.872	-22.752
Dipropyl ether	1.819	1.668	1.530	1.403	1.286	1.176	-28.761
Diisopropyl ether	1.508	1.371	1.243	1.127	1.021	0.919	-26.331
Dibutyl ether	2.375	2.190	2.021	1.866	1.721	1.584	-35.348
Acetone	2.452	2.303	2.164	2.037	1.917	1.806	-28.926
Pentan-2-one	2.947	2.765	2.598	2.441	2.297	2.161	-35.193
Pentan-3-one	2.938	2.757	2.588	2.430	2.286	2.149	-35.338
Butanal	2.507	2.348	2.201	2.064	1.941	1.824	-30.568
Acetonitrile	2.830	2.679	2.538	2.407	2.283	2.170	-29.577
1-Nitropropane	3.478	3.280	3.097	2.927	2.769	2.621	-38.370

^a Experimental gas-to-liquid partition coefficient data taken from Marciniak and Wlazło.²

Table 4. Logarithm of gas-to-([MeoeMPyrr]⁺[Tf₂N]⁻) partition coefficients at various temperatures and enthalpies of solvation (in kJ mol⁻¹)^a

Solute Temperature, K	logK _L						ΔH _{solv}
	318.15 K	328.15 K	338.15 K	348.15 K	358.15 K	368.15 K	kJ mol ⁻¹
Pentane	0.717	0.623	0.537	0.458	0.386	0.322	-17.685
Hexane	1.029	0.919	0.817	0.719	0.633	0.551	-21.422
3-Methylpentane	1.009	0.897	0.794	0.702	0.614	0.538	-21.093
2,2-Dimethylbutane	0.855	0.754	0.662	0.577	0.500	0.430	-19.036
Heptane	1.328	1.196	1.072	0.960	0.859	0.766	-25.159
Octane	1.623	1.476	1.336	1.210	1.093	0.984	-28.630
2,2,4-Trimethylpentane	1.326	1.196	1.076	0.965	0.860	0.768	-25.033
Nonane	1.920	1.747	1.589	1.444	1.310	1.188	-32.791
Decane	2.217	2.021	1.849	1.688	1.543	1.407	-36.186
Cyclopentane	1.146	1.037	0.941	0.851	0.769	0.694	-20.221
Cyclohexane	1.436	1.318	1.210	1.104	1.013	0.925	-22.900
Methylcyclohexane	1.591	1.459	1.336	1.225	1.124	1.033	-24.988
Cycloheptane	1.887	1.745	1.616	1.493	1.382	1.276	-27.333
Cyclooctane	2.288	2.124	1.975	1.833	1.707	1.587	-31.386
Pent-1-ene	0.938	0.834	0.740	0.656	0.574	0.504	-19.433
Hex-1-ene	1.248	1.127	1.017	0.913	0.822	0.735	-22.965
Cyclohexene	1.735	1.600	1.474	1.362	1.255	1.158	-25.801
Hept-1-ene	1.544	1.403	1.272	1.155	1.045	0.946	-26.747
Oct-1-ene	1.834	1.678	1.535	1.398	1.279	1.164	-30.000
Dec-1-ene	2.417	2.217	2.037	1.875	1.722	1.579	-37.417
Hex-1-yne	1.838	1.691	1.558	1.431	1.316	1.210	-28.134
Hept-1-yne	2.130	1.966	1.815	1.673	1.543	1.422	-31.742
Oct-1-yne	2.420	2.236	2.068	1.912	1.766	1.630	-35.323
Solute Temperature, K	logK _L						ΔH _{solv}
	318.15 K	328.15 K	338.15 K	348.15 K	358.15 K	368.15 K	kJ mol ⁻¹

Benzene	2.473	2.314	2.167	2.033	1.906	1.790	-30.556
Toluene	2.792	2.613	2.447	2.294	2.152	2.017	-34.664
Ethylbenzene	3.039	2.843	2.663	2.494	2.338	2.193	-37.874
<i>o</i> -Xylene	3.241	3.037	2.848	2.673	2.511	2.358	-39.558
<i>m</i> -Xylene	3.111	2.911	2.726	2.554	2.394	2.246	-38.744
<i>p</i> -Xylene	3.091	2.892	2.708	2.538	2.378	2.230	-38.554
Styrene	3.444	3.231	3.037	2.855	2.687	2.530	-40.911
α -Methylstyrene	3.625	3.398	3.188	2.992	2.808	2.637	-44.261
Thiophene	2.605	2.442	2.290	2.152	2.021	1.903	-31.487
Pyridine	3.293	3.103	2.927	2.763	2.611	2.470	-36.885
Methanol	2.176	2.033	1.903	1.780	1.668	1.562	-27.475
Ethanol	2.346	2.188	2.045	1.909	1.785	1.669	-30.297
Propan-1-ol	2.647	2.465	2.301	2.152	2.013	1.885	-34.069
Propan-2-ol	2.393	2.225	2.072	1.930	1.800	1.678	-31.990
Butan-1-ol	2.967	2.766	2.588	2.417	2.265	2.121	-37.832
Butan-2-ol	2.665	2.479	2.310	2.155	2.013	1.882	-34.994
2-Methyl-propan-1-ol	2.796	2.605	2.435	2.272	2.124	1.991	-36.062
<i>tert</i> -Butanol	2.415	2.236	2.076	1.928	1.792	1.671	-33.264
Water	2.473	2.318	2.176	2.045	1.922	1.813	-29.568
Methyl acetate	2.299	2.143	2.004	1.872	1.751	1.638	-29.535
Methyl propanoate	2.545	2.373	2.215	2.068	1.936	1.812	-32.829
Methyl butanoate	2.780	2.594	2.423	2.262	2.114	1.979	-35.938
Ethyl acetate	2.497	2.328	2.173	2.029	1.895	1.770	-32.544
Tetrahydrofuran	2.364	2.210	2.068	1.938	1.816	1.704	-29.528
1,4-Dioxane	3.027	2.841	2.670	2.511	2.362	2.223	-36.006
<i>tert</i> -Butyl methyl ether	1.672	1.534	1.408	1.290	1.182	1.083	-26.395
<i>tert</i> -Butyl ethyl ether	1.574	1.435	1.305	1.185	1.076	0.977	-26.763
<i>tert</i> -Amyl methyl ether	1.969	1.815	1.673	1.542	1.422	1.310	-29.515
Diethyl ether	1.369	1.250	1.140	1.037	0.943	0.856	-22.996
Dipropyl ether	1.790	1.639	1.504	1.377	1.260	1.152	-28.517
Diisopropyl ether	1.493	1.356	1.228	1.107	1.000	0.899	-26.642
Dibutyl ether	2.340	2.155	1.987	1.831	1.688	1.551	-35.271
Acetone	2.465	2.316	2.176	2.049	1.928	1.818	-29.028
Pentan-2-one	2.945	2.762	2.593	2.436	2.290	2.155	-35.390
Pentan-3-one	2.932	2.751	2.582	2.425	2.279	2.143	-35.373
Butanal	2.511	2.350	2.204	2.068	1.942	1.825	-30.665
Acetonitrile	2.853	2.700	2.558	2.425	2.301	2.185	-29.943
1-Nitropropane	3.488	3.290	3.107	2.936	2.777	2.630	-38.435

^a Experimental gas-to-liquid partition coefficient data taken from Marciniak and Wlazlo¹.

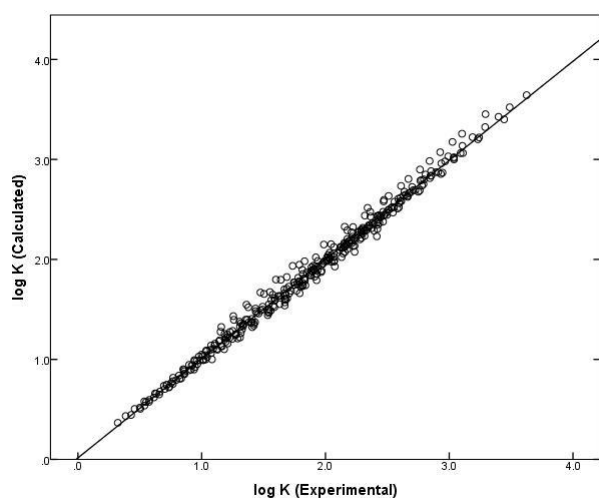


Figure 3. Graph of experimental logarithm of gas-to-([MeoeMPyrr]⁺[Tf₂N]⁻) partition coefficient ($\log K_L$) versus calculated $\log K_L$ based on Eqn. 20.

To determine the predictability of Eqn. 20, the data in Table 4 was also analyzed using a training set and test

analysis. Eqn. 23 is the resultant correlation from randomly splitting half of the $\log K_L$ data reported in Table 4. Using Eqn. 23 to predict the values in the test set yielded a $SD = 0.068$ log units, $AAE = 0.051$, and $AE = 0.007$. The very small difference in the coefficient values calculated between the training set and parent set show that the training set compounds and temperatures are representative of the parent compounds and temperatures. The low AE value shows very little bias between using Eqns. 20 and 23.

For comparison, the six temperature-specific Abraham model correlations developed by Marciniak and Wlazlo¹ for solutes dissolved in ([MeoeMPyrr]⁺[Tf₂N]⁻) had an average standard deviation of $SD=0.058$ log units. Each temperature specific correlation used six curve-fit equation coefficients. Equations 20 and 23 require far fewer equation coefficients and are able to describe the experimental data to within a standard deviation of less than 0.064 log units.

$$\log K_L = -10.280(0.514)/(2.303 R) + [2.246(12.310) - (48.518(4167)/T)] [E/(2.303 R)] +$$

$$\begin{aligned}
 & [3.492(14.742) - (-13094(4958)/T)] [S/(2.303 R)] + \\
 & [-30.517(16.211) - (23364(5530)/T)] [A/(2.303 R)] + \\
 & [-29.979(16.360) - (-11689(5524)/T)] [B/(2.303 R)] + \\
 & [-13.310(1.037) - (-7834(340)/T)] [L/(2.303 R)] \quad (23)
 \end{aligned}$$

$$N = 183, R^2 = 0.999, F = 15882, SD = 0.062 \text{ log units}$$

The removal of the c_H term from each of the three $\log K_L$ expressions and subsequent removal of $c_{H,solv}$ from the three ΔH_{solv} expressions is purely coincidental. Mintz, et al.⁴³ and Sprunger, et al.⁴⁴ have shown that temperature independent $\log K_L$ correlations for humic acid and polyurethane ether foam, respectively, produce twelve unique terms for all of the coefficients in Eqn. 11. The covariance encountered by the authors of this paper will most likely not occur with a data set that covers a much larger area of predictive space. In order to widen the area of predictive space, new partition coefficients will need to be determined for more acidic and more basic solutes.

CONCLUSIONS

Mathematical correlations are determined for predicting the gas-to-IL partition coefficients based on the Abraham solvation parameter model with temperature independent equation coefficients. The derived mathematical correlations (Eqns. 12, 16, and 20) are shown to provide reasonably accurate predictions the logarithm of the gas-to-IL partition coefficient for a wide variety of nonpolar and polar organic solutes dissolved in ([MHIm]⁺[B(CN)₄]⁻), ([MeoeMPip]⁺[Tf₂N]⁻), and ([MeoeMPyrr]⁺[Tf₂N]⁻) at temperatures from 318.15 K to 368.15 K to within a standard deviation of 0.077 log units or less. The success of the derived equations in predicting gas-to-ionic liquid partition coefficients suggests that the model can be used for other gas-to-condensed phase partitioning and for correlating gas chromatographic retention factor data measured at temperatures. As part of the present study, mathematical expressions (Eqns. 13, 17, and 21) were also derived for predicting the enthalpy of solvation for the dissolution of solutes in ([MHIm]⁺[B(CN)₄]⁻), ([MeoeMPip]⁺[Tf₂N]⁻), and ([MeoeMPyrr]⁺[Tf₂N]⁻) to within a standard deviation of 1.344 kJ/mol.

The method of regression analysis used in developing the log K_L correlations involved determining each of the equation coefficients solely from the measured gas-to-IL partition coefficient data. An alternative computational method could be to first regress the experimental ΔH_{solv} data, and then to insert the computed ΔH_{solv} equation coefficients into Eqn. 10. This would ensure identical values of $c_{H,solv}$, $e_{H,solv}$, $s_{H,solv}$, $a_{H,solv}$, $b_{H,solv}$ and $l_{H,solv}$ for both the log K_L and ΔH_{solv} correlations. This latter method was not pursued in the current study because our primary focus was in documenting the ability of Eqn. 10 to correlate gas-to-IL partition coefficient determined at different temperatures.

ACKNOWLEDGMENTS

Nishu Dabadge and Amy Tian thank the University of North Texas's Texas Academy of Math and Science (TAMS) program for a summer research fellowship. Bria Willis thanks the National Science Foundation for support received under NSF-REU grant (CHE-1004878).

REFERENCES

- Marciniak, A., Wlazło, M. *J. Chem. Thermodyn.*, **2012**, *54*, 90.
- Marciniak, A., Wlazło, M. *J. Chem. Thermodyn.*, **2012**, *49*, 137.
- Domańska, U., Lukoshko, E. V., Wlazło, M. *J. Chem. Thermodyn.*, **2012**, *47*, 389.
- Sprunger, L. M., Achi, S. S., Acree, W. E. Jr., Abraham, M. H. *Fluid Phase Equilib.*, **2010**, *288*, 139.
- Sprunger, L. M., Achi, S. S., Pointer, R., Acree, W. E. Jr., Abraham, M. H. *Fluid Phase Equilib.*, **2010**, *288*, 121.
- Abraham, M. H., Acree, W. E. Jr., Leo, A. J., Hoekman, D. *New J. Chem.*, **2009**, *33*, 568.
- Grubbs, L. M., Saifullah, M., De La Rosa, N. E., ye, S., Achi, S. S., Acree, W. E. Jr., Abraham, M. H. *Fluid Phase Equilib.*, **2010**, *298*, 48.
- Sprunger, L. M., Achi, S. S., Acree, W. E. Jr., Abraham, M. H., Leo, A. J., Hoekman, D., *Fluid Phase Equilib.*, **2009**, *281*, 144.
- Sprunger, L. M., Proctor, A., Acree, W. E. Jr., Abraham, M. H., Benjelloun-Dakhama, N. *Fluid Phase Equilib.*, **2000**, *270*, 30.
- Stephens, T. W., De La Rosa, N. E., Saifullah, M., Ye, S., Chou, V., Quay, A. N., Acree, W. E. Jr., Abraham, M. H. *Fluid Phase Equilib.*, **2011**, *308*, 64.
- Stephens, T. W., Quay, A. N., Chou, V., Loera, M., Shen, C., Wilson, A., Acree, W. E. Jr., Abraham, M. H. *Glob. J. Phys. Chem.*, **2012**, *1/1*.
- Stephens, T. W., Wilson, A., Dabadge, N., Tian, A., Hensley, H. J., Zimmerman, M., Acree, W. E. Jr., Abraham, M. H. *Glob. J. Phys. Chem.*, **2012**, *3*, 9/1.
- Sprunger, L. M., Gibbs, J., Acree, W. E. Jr., Abraham, M. H. *QSAR Comb. Sci.*, **2009**, *28*, 72.
- Sprunger, L., Acree, W. E. Jr., Abraham, M. H. *J. Chem. Inf. Model.*, **1997**, *47*, 1808.
- Abraham, M. H., Ibrahim, A., Acree, W. E. Jr. *Eur. J. Med. Chem.*, **2008**, *43*, 478.
- Abraham, M. H., Ibrahim, A., Acree, W. E. Jr. *Eur. J. Med. Chem.*, **2007**, *42*, 743.
- Sprunger, L. M., Gibbs, J., Acree, W. E. Jr., Abraham, M. H. *QSAR Comb. Sci.*, **2008**, *27*, 1130.
- Bowen, K. R., Flanagan, K. B., Acree, W. E. Jr., Abraham, M. H., Rafols, C. *Sci. Total Environ.*, **2006**, *371*, 99.
- Bowen, K. R., Flanagan, K. B., Acree, W. E. Jr., Abraham, M. H. *Sci. Total Environ.*, **2006**, *369*, 109.
- Hoover, K. R., Flanagan, K. B., Acree, W. E. Jr., Abraham, M. H. *J. Environ. Eng. Sci.*, **2007**, *6*, 165.
- Hoover, K. R., Acree, W. E. Jr., Abraham, M. H. *Chem. Res. Toxicol.*, **2005**, *18*, 1497.
- Anderson, J. L., Ding, J., Welton, T., Armstrong, D. W. *J. Am. Chem. Soc.*, **2002**, *124*, 14247.
- Domańska, U., Krolikowska, M., Acree, W. E. Jr., Baker, G. A., *J. Chem. Thermodyn.*, **2011**, *43*, 1050.
- Mutelet, F., Revelli, A.-L., Jaubert, J.-N., Sprunger, L. M., Acree, W. E. Jr., Baker, G. A. *J. Chem. Eng. Data*, **2010**, *55*, 234.

- ²⁵Stephens, T. W., Acree, W. E. Jr., Twu, P., Anderson, J. L., Baker, G. A., Abraham, M. H. *J. Solution Chem.*, **2012**, *41*, 1165.
- ²⁶Twu, P., Anderson, J. L., Stephens, T. W., Acree, W. E. Jr., Abraham, M. H. *Eur. Chem. Bull.*, **2012**, *1*, 212.
- ²⁷Jiang, R., Anderson, J. L., Stephens, T. W., Acree, W. E., Abraham, M. H. *Eur. Chem. Bull.*, **2013**, *2*, 741.
- ²⁸Abraham, M. H., Acree, W. E. Jr., *J. Solution Chem.*, **2011**, *40*, 1279.
- ²⁹Mintz, C., Gibbs, J., Acree, W. E. Jr., Abraham, M. H. *Thermochim. Acta*, **2009**, *484*, 65.
- ³⁰Mintz, C., Burton, K., Ladlie, T., Clark, M., Acree, W. E. Jr., Abraham, M. H. *J. Mol. Liq.*, **2009**, *144*, 23.
- ³¹Mintz, C., Ladlie, T., Burton, K., Clark, M., Acree, W. E. Jr., Abraham, M. H. *QSAR Comb. Sci.*, **2008**, *27*, 627.
- ³²Mintz, C., Burton, W. E. Jr., Abraham, M. H., *QSAR Comb. Sci.*, **2008**, *27*, 179.
- ³³Stephens, T. W., Chou, V., Quay, A. N., Acree, W. E. Jr., Abraham, M. H., *Thermochim. Acta*, **2011**, *519*, 103.
- ³⁴Stephens, T. W., De La Rosa, N. E., Saifullah, M., Ye, S., Chou, V., Quay, A. N., Acree, W. E. Jr., Abraham, M. H. *Thermochim. Acta*, **2011**, *523*, 214.
- ³⁵Abraham, M. H., Whiting, G. S., Doherty, R. M., Shuely, W. J. *J. Chem. Soc., Perkin Trans. 2*, **1990**, 1451.
- ³⁷Abraham, M. H., Grellier, P. L., Prior, D. V., Duce, P. P., Morris, J. J., Taylor, P. J. *J. Chem. Soc., Perkin Trans. 2*, **1989**, 699.
- ³⁸Abraham, M. H., Grellier, P. L., Prior, D. V., Morris, J. J., Taylor, P. J., *J. Chem. Soc., Perkin Trans. 2*, **1990**, 521.
- ³⁹Abraham, M. H., McGowan, J. C. *Chromatographia*, **1987**, *23*, 243.
- ⁴⁰Abraham, M. H., Grellier, P. L., McGill, R. A., *J. Chem. Soc., Perkin Trans 2*, **1987**, 797.
- ⁴¹Sprunger, L. M., Gibbs, J., Proctor, A., Acree, W. E. Jr., Abraham, M. H., Meng, Y., Yao, C., Anderson, J. L. *Ind. Eng. Chem. Res.*, **2009**, *48*, 4145.
- ⁴²Grubbs, L. M., Saifullah, M., De La Rosa, N. E., Acree, W. E. Jr., Abraham, M. H., Zhao, Q., Anderson, J. L., *Glob. J. Phys. Chem.*, **2010**, *1*, 1.
- ⁴³Grubbs, L. M., Ye, S., Saifullah, M., McMillan-Wiggins, M. C., Acree, W. E. Jr., Abraham, M. H. *Fluid Phase Equilibr.*, **2011**, *301*, 257.
- ⁴⁴Mintz, C., Ladlie, T., Burton, K., Clark, M., Acree, W. E. Jr., Abraham, M. H., *QSAR Comb. Sci.*, **2008**, *27*, 483.
- ⁴⁵Sprunger, L., Acree, W. E. Jr., Abraham, M. H. *Anal. Chem.*, **2007**, *79*, 6891.

Received: 01.06.2013.

Accepted: 03.07.2013.